ELSEVIER

Chemical Engineering Journal 85 (2002) 99–109

Chemical Engineering Journal

www.elsevier.com/locate/cej

Influence of cell construction on the electrochemical reduction of nitrate

M. Paidar [a], K. Bouzek [a,*], H. Bergmann [b]

[a] *Department of Inorganic Technology, Institute of Chemical Technology, Technická 5, 166 28 Prague 6, Czech Republic*
[b] *Anhalt University of Applied Sciences, Bernburger Straße 55, D-06366 Köthen, Germany*

Received 17 January 2001; accepted 6 April 2001

Abstract

The electrochemical reduction of nitrates in the weakly alkaline electrolyte, simulating spent solution after regeneration of a strongly basic anion exchanger was studied. Copper was used as the cathode material. The influence of the electrolyser construction, cathode form and process parameters on the current efficiency of the nitrate reduction was followed. Four types of cell construction were used: a plate-electrode cell, a cell with a fluidised bed of inert particles in the inter-electrode space, a packed bed cathode cell and a vertically moving particle bed cell. The highest current efficiency with respect to the nitrate reduction was observed for the vertically moving particle bed reactor. On the other hand, unexpectedly high efficiency was also observed for the simple plate-electrode cell, the disadvantage being very low current density (below 40 A m^{-2}) resulting in suitable behaviour. From the point of view of cell efficiency coupled with simplicity of construction and operation, the optimal cell seems to be the cell with the fluidised bed of inert particles in the inter-electrode space.

Keywords: Nitrates; Reduction; Cathode; Cell type; Alkaline solution

1. Introduction

Cathodic nitrate reduction is an interesting problem both from a theoretical and an applied research point of view. This is mainly because the reaction mechanism of this process is not well understood so far and because nitrate is a serious environmental pollutant. The main source of nitrate in water is the excessive application of agricultural fertilisers. This caused the penetration of large quantities of nitrate into underground and surface water [1–3]. The high concentration of nitrates in water has a detrimental effect on the environment and also constitutes a problem in water for industrial use.

Besides the treatment of drinking and industrial water, the necessity of dealing with large amounts of alkaline waste water with a high nitrate content from the nuclear industry has initiated renewed intensive interest in this problem on the part of electrochemical engineers in the last decade [4,5].

Nowadays in drinking water treatment ion exchange represents the most widespread method for the removal of nitrates [6]. To regenerate saturated ion-exchangers a high excess of regeneration agent (commonly NaCl) has to be used. Consequently, the salinity of wastewater originating from this process increases substantially. In addition, the nitrate released from the ion-exchanger contaminates the regenerating solution, and thus, returns into the environment. Therefore, a means of removal nitrate in a closed cycle stream is being investigated [7].

Beside other methods (e.g. application of micro-organisms [6,8] and heterogeneous catalysis [6,9]), frequent reference is made in the literature to selective electrochemical reduction as a method for the reduction of nitrates to nitrogen and ammonia [4,10,11]. In contrast to alternative methods, this is a relatively simple technology consisting of a minimum number of steps. Moreover, it is suitable for treating the spent regeneration solutions from the ion-exchange columns. This is because electrochemical treatment does not substantially influence the quality of the regeneration solution, which would hinder its reuse in a closed circle.

The following reactions may be considered to proceed on the cathode during electrolysis [12]:

$$NO_3^- + H_2O + 2e^- = NO_2^- + 2OH^- \quad (1)$$

$$NO_3^- + 3H_2O + 5e^- = \tfrac{1}{2}N_2 + 6OH^- \quad (2)$$

$$NO_3^- + 6H_2O + 8e^- = NH_3 + 9OH^- \quad (3)$$

$$NO_2^- + 2H_2O + 3e^- = \tfrac{1}{2}N_2 + 4OH^- \quad (4)$$

$$NO_2^- + 5H_2O + 6e^- = NH_3 + 7OH^- \quad (5)$$

$$NO_2^- + 4H_2O + 4e^- = NH_2OH + 5OH^- \quad (6)$$

* Corresponding author.
E-mail address: bouzekk@vscht.cz (K. Bouzek).

1385-8947/02/$ – see front matter
PII: S1385-8947(01)00158-9

Nomenclature

a	specific surface (m^{-1})
d	diameter (m)
D	diffusion coefficient ($m^2\,s^{-1}$)
h	thickness of the packed bed electrode (m)
$\bar{j}_b$	average current density for the 3D electrode in flow-by arrangement ($A\,m^{-2}$)
$\bar{j}_t$	total current density for the 3D electrode in flow-through arrangement ($A\,m^{-2}$)
k	mass-transfer coefficient ($m\,s^{-1}$)
L	length (height) of the electrode (m)
Re	Reynolds number $Re = d_e v/\nu'$
Sc	Schmidt number $Sc = \nu'/D$
Sh	Sherwood number $Sh = kd_e/D$
$\dot{v}$	superficial fluid velocity ($m\,s^{-1}$)
j_D	mass-transfer factor Eq. (13)

Greek letters

ε	porosity
ν'	kinematic viscosity ($m^2\,s^{-1}$)
τ	time (s)

Subscripts

e	equivalent value
p	particle
0	bulk value

Only typical overall reactions providing stable products are given here. The spectrum of possible intermediate steps is much broader. However, this exceeds the scope of this study. Hydrogen evolution (Eq. (7)) is the main parasitic cathodic reaction.

$$2H_2O + 2e^- = H_2 + 2OH^- \quad (7)$$

Oxygen evolution is the main anodic reaction (Eq. (8)).

$$4OH^- = O_2 + 2H_2O + 4e^- \quad (8)$$

The desired cathodic process is the reduction of nitrate to nitrogen according to Eq. (2). According to the literature data [13], however, nitrate reduction mainly follows Eq. (3) and the process requires eight electrons. This is in agreement with our previous [14] and our present results. The overall process of nitrate reduction in an electrochemical cell may then be described by Eq. (9).

$$NaNO_3 + 2H_2O = NH_3 + 2O_2 + NaOH \quad (9)$$

During electrolysis the electrolyte gradually becomes alkaline Eq. (9). Hence, $NaHCO_3$ present in the solution (for the composition of the solution see below) is converted to carbonate. Adding this process to Eq. (9), the overall cell reaction, Eq. (10), is obtained:

$$NaNO_3 + NaHCO_3 + H_2O = NH_3 + 2O_2 + Na_2CO_3 \quad (10)$$

In the present study, copper was used as the cathode material since it has been identified as having high electrocatalytic activity for nitrate reduction in strongly alkaline media [5] as well as in hydrogen carbonate solutions [14,15].

Originally, the electrochemical reduction of nitrates was studied mainly in acidic solutions [16–19]. These studies focus mainly on the reaction mechanism. Voltammetry is the main technique applied. At present research in this field focuses on alkaline solutions. The reason is the large quantities of strongly alkaline wastewater from the nuclear industry to be treated. One part of the papers published on the problem of electrochemical nitrate reduction is devoted to the voltammetric study of the reaction mechanism using different cathode materials [10,13,15,20,21]. Other studies deal with nitrate reduction electrolysis [4,5,14,22,23] with respect to products, current efficiency, etc. In most cases, cells equipped with plate-electrodes were used [5,14,22,23]. Some of the authors have applied packed bed cathodes to reduce nitrate [4]. This was mainly because a low nitrate outlet concentration has to be obtained. Up to now, however, no study dealing with the influence of the cell, and particularly the cathode construction, on process efficiency has been made. The aim of this work is to fill this gap.

Concentrated $NaHCO_3$ solution was used as an electrolyte in this study. It is because HCO_3^- ions are more suitable for drinking water treatment when compared to Cl^- or SO_4^{2-} [24]. Four electrochemical cells were compared: plate-electrodes, cell with fluidised bed of inert particles in the inter-electrode space, packed bed cathode and vertically moving particle bed (VMPB) [25].

2. Evaluation of the mass-transfer coefficients

Since we are dealing with highly diluted solutions, mass-transfer to the cathode surface is expected to play an important role in the behaviour of the respective cell type. Therefore, the mass-transfer coefficients have to be evaluated in order to discuss the results obtained experimentally.

The mass-transfer coefficient k value for the electrolyte laminar flow in the empty channel between the plate-electrodes can be evaluated by Eq. (11) proposed by Roušar et al. [26].

$$Sh = 1.85\left(\frac{d_e}{L} Re\, Sc\right)^{1/3} \quad (11)$$

For the mass-transfer to the plate-electrodes immersed into the fluidised bed of inert particles Eq. (12) was proposed [27].

$$j_D \varepsilon = 0.28\left(\frac{Re_{d_p}}{1-\varepsilon}\right)^{-0.36} \quad (12)$$

where

$$j_D = \frac{k}{v} Sc^{2/3} \quad (13)$$

$$Re_{d_p} = \frac{d_p v}{\nu'_e} \tag{14}$$

In the case of the 3D electrode, the variation of the electroactive species concentration along the electrode has to be considered. In order to evaluate concentration as a function of the position, we start with the mass balance.

$$\mathrm{d}c_y = -akc_y \,\mathrm{d}\tau \tag{15}$$

where

$$\mathrm{d}\tau = \frac{\mathrm{d}y}{v} \tag{16}$$

By substituting $\mathrm{d}\tau$ from Eq. (15) in Eq. (16), we obtain

$$\frac{\mathrm{d}c_y}{c_y} = -\frac{ak}{v}\mathrm{d}y \tag{17}$$

By integrating Eq. (17) in the range of c_0 to c_y and of $y = 0$ to y, after rearrangement, we obtain

$$c_y = c_0 \exp\left(-\frac{ak}{v}y\right) \tag{18}$$

The local current density can be calculated as

$$j_y = nFahkc_y \tag{19}$$

The average current density is given by integration according to Eq. (20).

$$\bar{j}_b = \frac{1}{L}\int_0^L j_y \,\mathrm{d}y \tag{20}$$

This yields

$$\bar{j}_b = \frac{nFhv}{L}c_0\left[1 - \exp\left(-\frac{ak}{v}L\right)\right] \tag{21}$$

The mass-transfer coefficient k was calculated using the correlation for 3D electrodes referred to by Storck et al. [28].

$$k = 1.875 v Re_p^{-0.55} Sc^{-2/3} \tag{22}$$

The mass-transfer in the VMPB cathode was not studied in detail and no regression for its evaluation is known so far. However, since the drum rotation rate is relatively slow (0.05 Hz), at this stage this type of electrode may considered to be described with satisfactory accuracy by the equations valid for the stationary 3D electrode. In the case of the VMPB cell, the general flow direction of electrolyte is parallel to the current lines. Radial convection of the electrolyte induced by the cathode rotation is neglected. Therefore, relationships different from Eqs. (19) and (20) have to be used to calculate the average current density at the terminal electrode. In this case, Eq. (18) is also used to evaluate the dependence of the concentration of the electroactive species on the position in the electrode. The local value of the current density can now be expressed as follows.

$$j_y = nFakc_y \tag{23}$$

Total current density may be obtained by integrating the local current density across the electrode according to Eq. (24)

$$\bar{j}_b = \int_0^L j_y \,\mathrm{d}y \tag{24}$$

By substituting j_y from Eq. (23) in Eq. (24) and consequently c_y from Eq. (18) in Eq. (23) and simple rearrangement we obtain an expression for the current density at the terminal electrode for the electrolyte flow parallel to the current lines.

$$\bar{j}_b = nFvc_0\left[1 - \exp\left(-\frac{ak}{v}h\right)\right] \tag{25}$$

Since hydrodynamic conditions in the cathode are in this case out of the range of validity of Eq. (22), the mass-transfer coefficient was in this case calculated using a correlation proposed by Colquhoun-Lee and Stepanek [29] and recommended by Newman and Tiedemann [30].

$$k = 0.62aD\left(\frac{v}{av'}\right)^{0.61} Sc^{1/3} \tag{26}$$

3. Experimental

3.1. Apparatus

The following types of cell were used: plate-electrodes, plate-electrodes with fluidised bed of inert particles in the inter-electrode space, packed bed cathode and VMPB cathode cell. Schematic sketch of the individual cells constructions are shown in Fig. 1A–D.

The construction of the plate-electrode cell (Fig. 1A) was identical to those used in the previous work [14]. The only difference was that the number of electrodes was raised to five cathodes and six anodes.

The construction of the electrolytic cell with the fluidised bed of inert particles (Fig. 1B) was close to that of plate-electrodes. The dimensions of the electrodes were 0.06 m × 0.30 m. The cell was equipped with the two anodes and one cathode. The glass spheres 1×10^{-3} m in diameter formed a fluidised bed. In this study, bed expansion of 50% was used. This was because it provides the highest mass-transfer enhancement [27].

Flow-by (current lines perpendicular to the electrolyte flow direction) arrangement was used for the packed bed cathode (Fig. 1C). The dimensions of the anode and cross-section of the cathode were 0.05 m × 0.10 m. The bed consisted of Cu spheres 3×10^{-3} m in diameter. The depth of the cathode was 0.01 m. As a support for the packed bed a PVC diaphragm was used. The hydraulic circles were not separated and a joint electrolyte reservoir was used.

The VMPB cell used last (Fig. 1D) is described in more detail in [25]. The cell used consisted of six cathode chambers first 0.04 m and remaining 0.03 m thick and 0.175 m in diameter. The rotation rate of the cathode chambers was 2.8 revolutions per minute. The main particle diameter

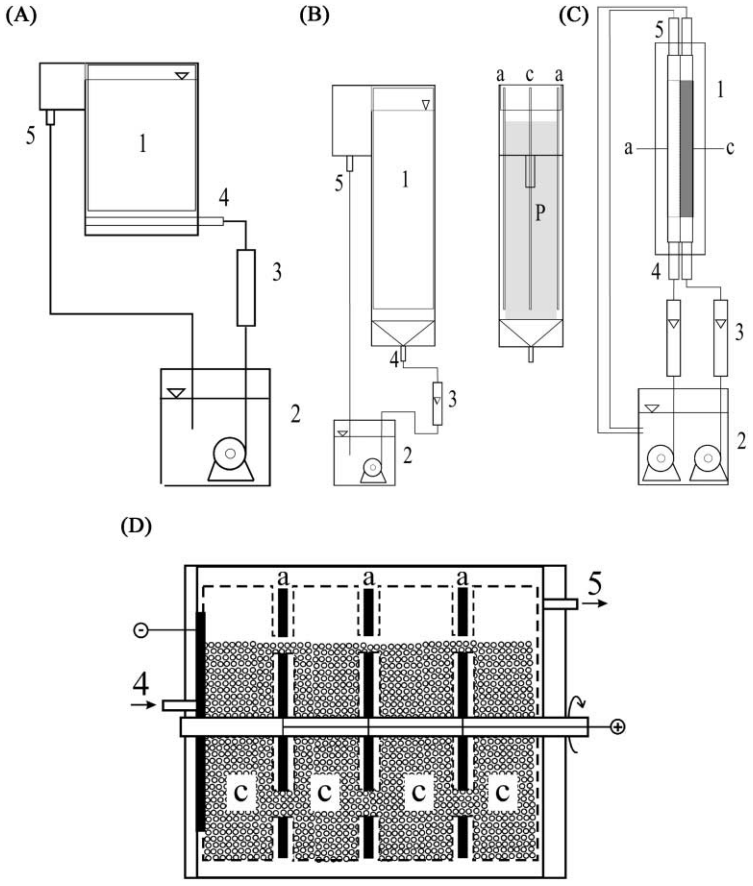

Fig. 1. Schematic sketch of electrochemical cells used. (A) Plate-electrodes cell, (B) cell with fluidising bed of inert particles, (C) packed bed cathode cell, and (D) VMPB cathode cell. 1: electrolytic cell; 2, 3: electrolyte reservoir and flow meter; 4, 5: electrolyte inlet and outlet; a—anode; c—cathode; P—inert particles.

was 2×10^{-3} m. Seventy percent of the cathode chamber cross-section was filled with particles. Flow-through (current lines parallel to the electrolyte flow) cathode construction was used in this cell.

Copper was used as the cathode material in all the types of cell. The electrodes were degreased and cleaned in diluted (1:1) HNO_3 before the start of the first electrolysis. Between electrolysis runs the cathodes were left immersed in the electrolyte solution. No additional cathode treatment was provided between the individual experiments.

Activated Ti anodes were used during all experiments in this study. The temperature was maintained at 20 °C by a thermostat.

All potentials in the text refer to the SCE electrode.

3.2. Chemicals

An electrolyte simulating spent solution after strongly basic anion exchanger regeneration was used throughout this study. Its composition was as follows: 84.0 g dm^{-3} $NaHCO_3$, 0.4 g dm^{-3} NaCl, 0.4 g dm^{-3} Na_2SO_4 and 1.0 g dm^{-3} NO_3^- (as $NaNO_3$). The following transport parameters of the solution were used for the calculations: kinematic viscosity of the 84 g dm^{-3} $NaHCO_3$ solution $\nu' = 1.193 \times 10^{-6}$ m^2 s^{-1}, nitrate ion and oxygen diffusion coefficients were approximated by their values in water $D_{NO_3} = 1.9 \times 10^{-9}$ m^2 s^{-1} and $D_{O_2} = 2.3 \times 10^{-9}$ m^2 s^{-1}.

3.3. Analytical methods

Samples were taken at regular intervals and were analysed for NO_3^-, NO_2^-, NH_3 and pH. The determination of nitrate content was based on light absorption at 210 nm [31]; nitrite was allowed to react with sulfanilic acid and α-naphthol in a weakly acidic solution yielding an orange-coloured azo dyestuff with absorption maximum at 480 nm [31]. Ammonia was determined by the Nessler method [31].

4. Results

The electrochemical reduction of nitrates was primarily studied using a cell with plate-electrodes. The results for the different cathodic current densities are given in Fig. 2. The electrical charge per volume of solution treated is used instead of time as the *x*-axis. This made it easier to compare

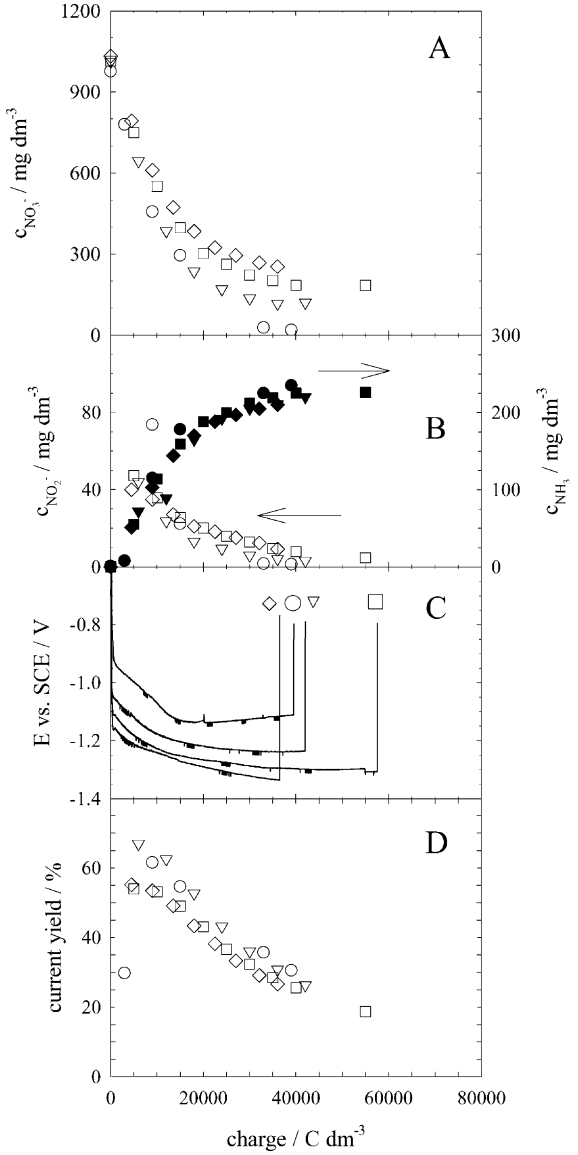

Fig. 2. Electrochemical reduction of nitrates in the plate-electrodes cell. Dependence of (A) nitrates concentration, (B) nitrites (empty symbols) and ammonium (filled symbols), (C) cathode potential, and (D) current yield with respect to the nitrates reduction on the electrical charge per unit volume of the electrolyte. Cathodic current density: (○) 20 A m^{-2}, (▽) 40 A m^{-2}, (□) 50 A m^{-2} and (◇) 60 A m^{-2}. Temperature 20 °C, electrolyte without the addition of Cu ions.

the results obtained using different types of electrochemical cells characterised by different total electrode areas and electrolyte volumes. As follows from the figure, in the current density range studied (20–60 A m^{-2}) the behaviour of the system does not vary dramatically. Two main differences are the increase in average potential and the limiting value of the nitrate concentration in the solution after electrolysis. The concentration reached a value of 18 mg dm^{-3} at a current density of 20 A m^{-2} and increased to a value of 254 mg dm^{-2} at a current density of 60 A m^{-2}. This is a very important parameter from the point of view of the regeneration of the ion exchange columns. It was estimated experimentally that, in order to assure a satisfactorily efficient regeneration and to minimise the volume of the regeneration solution needed, the concentration of nitrate in the regeneration solution after electrolysis should not exceed approximately 100–150 mg dm^{-3}. Nevertheless, concentration below 50 mg dm^{-3} is preferred [24]. This result was obtained within the electrolysis time under study only using a current density equal or lower than 40 A m^{-2}. The situation with nitrite concentration is similar and a concentration of about one order of magnitude higher was obtained using the current density of 60 A m^{-2} when compared to the concentration of about 1 mg dm^{-3} reached at 20 A m^{-2}. Since nitrite is an even more dangerous pollutant than nitrate and its limit in drinking water is set at 0.5 mg dm^{-3} [32], this is also a very important parameter.

It is interesting to note the potential step apparent on the chronopotentiometric curves. Although, this appears at all the current densities studied, it is most apparent at the lowest one. This process is connected with the mass-transfer phenomenon at the cathode surface, as discussed below.

As reported previously for the more diluted sodium hydrogen carbonate solution [14], a substantial improvement to the plate-electrode cell behaviour may be brought about by adding the copper carbonate to the solution. Fig. 3 shows the behaviour of this system. The most apparent difference, when compared to electrolysis without the addition of Cu ions to the solution, is the less cathodic and more stable potential of the Cu electrode. This varies in a range of −0.95 to −1.1 V for the current density range studied. The concentration of nitrite in the solution also corresponds to this fact. Compared with the case without an addition of Cu ions, this is five times higher. The increase in the electrocatalytic activity of the cathode is demonstrated by the slightly higher current yields obtained. More important, however, is the lower value of the nitrate end concentration obtained. For the electrolyte with an addition of Cu ions end concentration of 70 mg NO_3^- dm^{-3} and without an addition of Cu 260 mg NO_3^- dm^{-3} was reached at a current density of 60 A m^{-2}. This is in good agreement with the observations made using cyclic voltammetry, which will be discussed later.

Since we are dealing with a low concentration of the electroactive species in the electrolyte, the application of systems with enhanced mass-transfer is obvious. Therefore, the plate-electrodes cell with a fluidised bed of inert particles in the inter-electrode space was next to be studied. Simple construction and maintenance, together with intensive mass-transfer and mechanical abrasion of the cathode surface are characteristic of this type of cell. Fig. 4 shows the results obtained for the 50% fluidised bed expansion and various cathode current densities. The results for this type of cell are in some respects similar to the plate-electrode cell. The changes in the dependencies observed are, however, more sudden, and thus, more pronounced. The nitrate concentration is reduced to 50 mg dm^{-3} with a

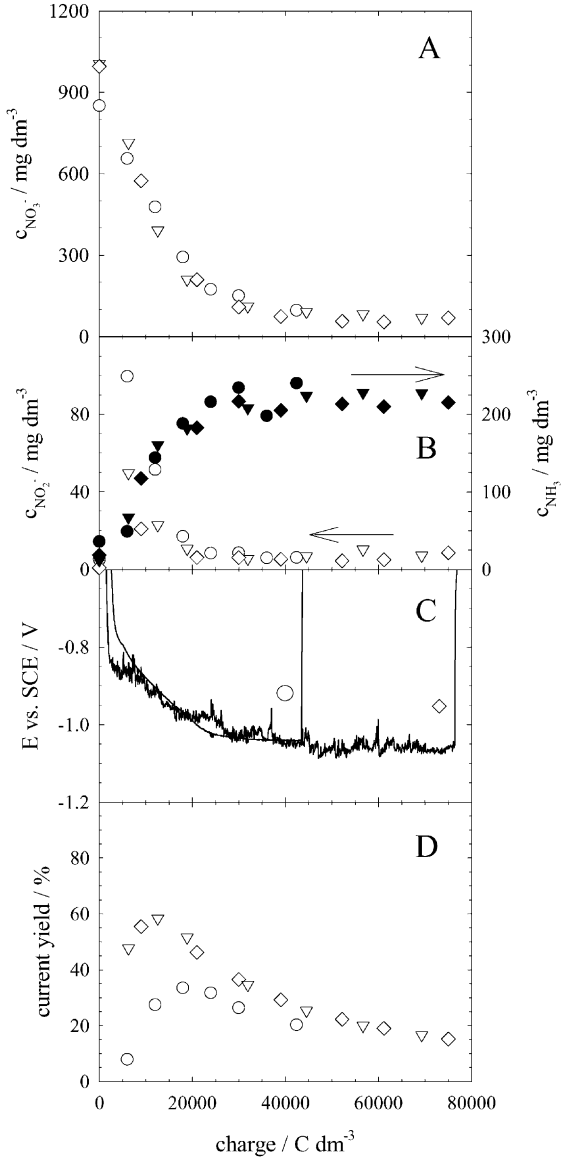

Fig. 3. Electrochemical reduction of nitrates in the plate-electrode cell. Dependence of (A) nitrates concentration, (B) nitrites (empty symbols) and ammonium (filled symbols), (C) cathode potential, and (D) current yield with respect to the nitrate reduction on the electrical charge per unit volume of the electrolyte. Cathodic current density: (○) 20 A m^{-2}, (▽) 40 A m^{-2} and (◇) 60 A m^{-2}. Temperature 20 °C, electrolyte with the addition of $CuCO_3$.

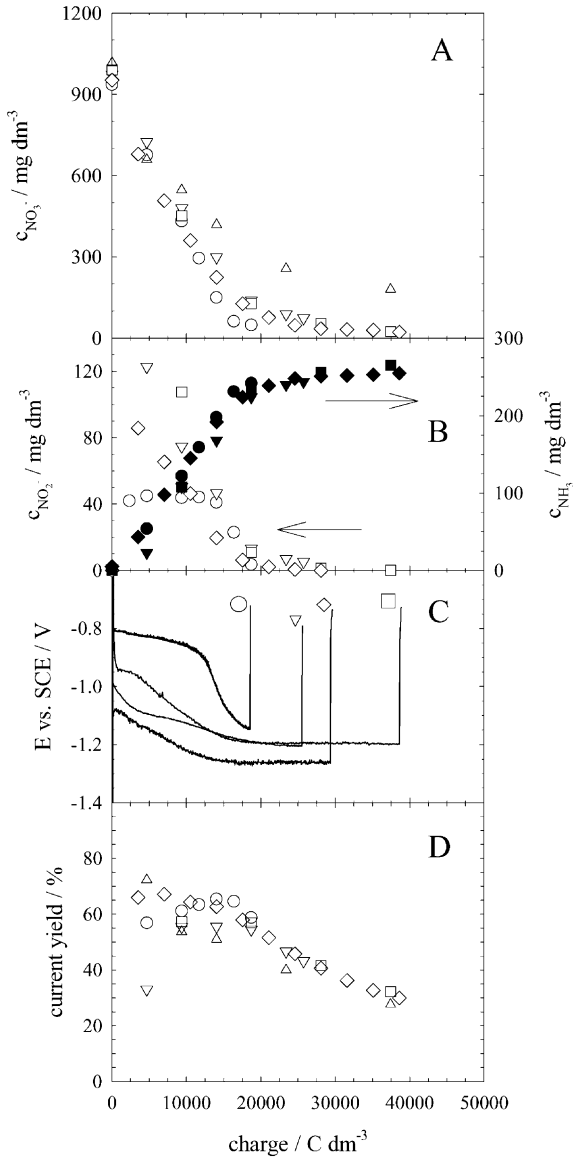

Fig. 4. Electrochemical reduction of nitrates in the cell with the fluidised bed of inert particles in the inter-electrode space. Dependence of (A) nitrate concentration, (B) nitrites (empty symbols) and ammonium (filled symbols), (C) cathode potential, and (D) current yield with respect to the nitrate reduction on the electrical charge per unit volume of the electrolyte. Cathodic current density: (○) 20 A m^{-2}, (▽) 40 A m^{-2}, (□) 80 A m^{-2}, (◇) 120 A m^{-2} and (△) 320 A m^{-2}. Temperature 20 °C, electrolyte without the addition of Cu ions.

current efficiency of about 45% even at a current density of 120 A m^{-2}.

The most widespread method of treating diluted solutions in the literature is the application of 3D electrodes. The packed bed cathode in the form of a stationary layer of copper spheres was applied in our case, for results see Fig. 5. The concentration of nitrate in the solution did not decrease below 80 mg dm^{-3} in the electrolysis duration range under study. Moreover, at the lowest superficial current density used (100 A m^{-2}) the current yield of the process was apparently lower when compared to the higher current loads. On the other hand, the trend of the concentration in the whole current density range under study still decreases with electrolysis time, indicating a further decrease in nitrate concentration to a value as close to zero as possible. Application of the 3D cathode leads simultaneously to an increase in the maximum nitrite concentration in the solution. This indicates lower real current densities (at least in part of the cathode) when compared to the plate-electrode, as will be discussed later.

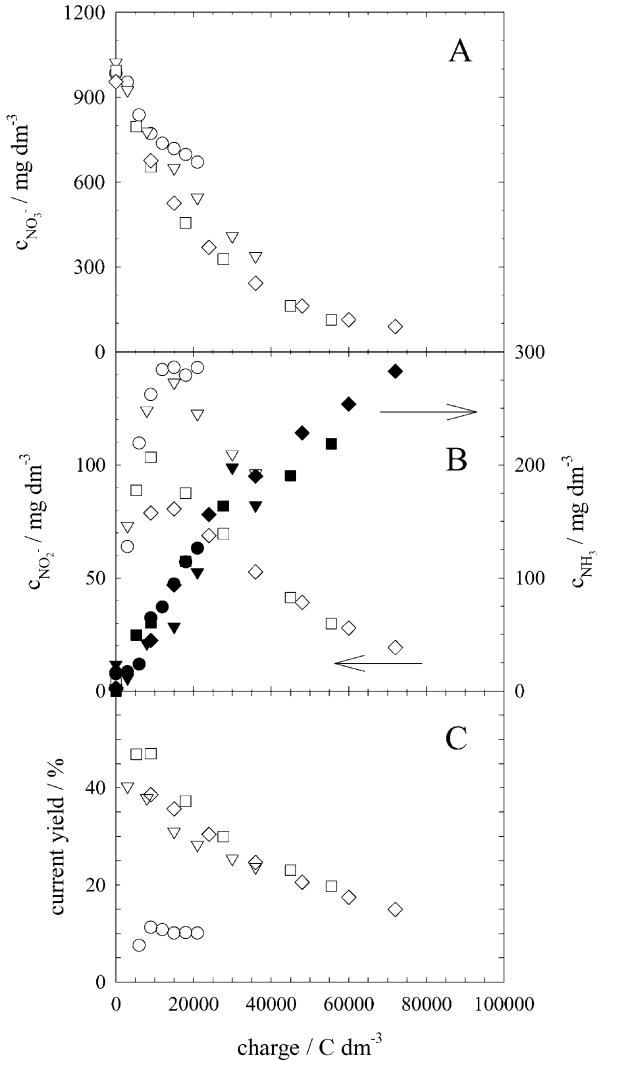

Fig. 5. Electrochemical reduction of nitrates in the cell with packed bed cathode (flow-by arrangement). Dependence of (A) nitrate concentration, (B) nitrites (empty symbols) and ammonium (filled symbols), and (C) current yield with respect to the nitrate reduction on the electrical charge per unit volume of the electrolyte. Cathodic current density with respect to the current collector: (○) 100 A m^{-2}, (▽) 200 A m^{-2}, (□) 300 A m^{-2} and (◇) 400 A m^{-2}. Temperature 20 °C, electrolyte without the addition of $CuCO_3$.

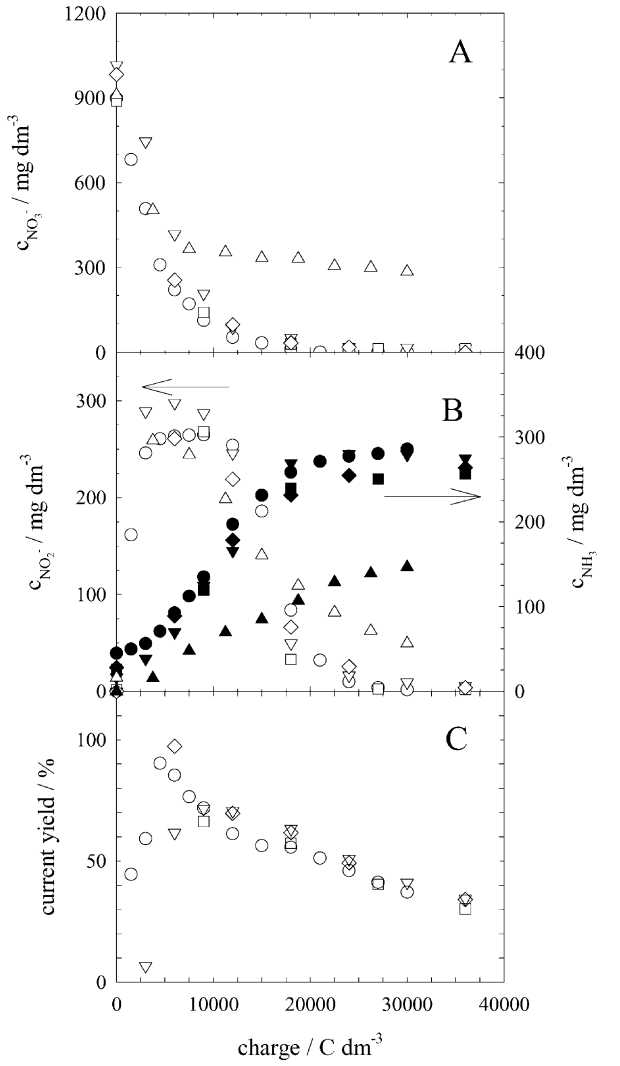

Fig. 6. Electrochemical reduction of nitrates in the VMPB cathode cell. Dependence of (A) nitrate concentration, (B) nitrites (empty symbols) and ammonium (filled symbols), and (C) current yield with respect to the nitrate reduction on the electrical charge per unit volume of the electrolyte. Total current through the cell: (○) 5 A, (▽) 10 A, (□) 15 A, (◇) 20 A and (△) 25 A. Temperature 20 °C, electrolyte without the addition of $CuCO_3$.

A more sophisticated arrangement of the 3D copper cathode is that of the VMPB cathode cell. The main differences when compared to the packed bed cell are the application of the rotating particle cathode and flow-through arrangement of the cathode (current lines parallel to the electrolyte flow). Cathode rotation provides more intensive electrolyte mixing, and thus, enhances mass-transfer between the electrolyte and the electrode surface. An additional effect observed is the mechanical renewal of the cathode surface by the permanent mechanical friction among the neighbouring particles. The results obtained using this type of cell are shown in Fig. 6. As is apparent, the current efficiencies reached values much higher than in the previous two types of cell. Correspondingly, the final concentration of nitrates in the solution decreased with satisfactory current efficiency of about 60% below 50 mg dm^{-3}. An important difference is the further increase in the maximum nitrite concentration in the solution when compared to the previous two types of cell.

5. Discussion

The individual electrolytic cells are compared with respect to theirs calculated mass-transfer limited current densities for the nitrate reduction reaction and experimentally determined current densities providing nitrate concentration reduction below 50 mg dm^{-3} required for efficient ion exchanger regeneration in Table 1. The parameters for which

Table 1
Comparison of the individual electrochemical cells studied

Cell type	k_{NO_3} ($m\,s^{-1}$)	Calculated mass-transfer limited current density ($A\,m^{-2}$)	Experimentally determined current density providing effective reduction[a] ($A\,m^{-2}$)
Parallel plate-electrodes	3.4×10^{-6}	42	20
Fluidised bed of inert particles	3.0×10^{-5}	373	160
Flow-by packed bed cathode	8.3×10^{-5}	11000	–[b]
VMPB cathode	1.5×10^{-5} [c]	19060	1430

[a] Highest current density providing nitrate concentration reduction below $50\,mg\,dm^{-3}$ required for sufficient ion exchanger regeneration.
[b] Nitrate concentration below $50\,mg\,dm^{-3}$ was not reached within the experimental conditions used.
[c] Approximate value calculated using packed bed electrode correlation.

these values were obtained are discussed in more detail for each particular case below.

For the plate-electrode cell the linear flow rate of the electrolyte in the inter-electrode channel of $4.5 \times 10^{-3}\,m\,s^{-1}$ was used. The equivalent diameter of the channel was $1.14 \times 10^{-2}\,m$. For these values, using Eq. (11), a mass-transfer coefficient value of $k_{NO_3} = 3.4 \times 10^{-6}\,m\,s^{-1}$ was calculated. Considering the concentration of nitrates at the beginning of the electrolysis (i.e. $1\,g\,dm^{-3}$) and reduction to proceed according to Eq. (3), the limiting current density for the nitrate reduction was calculated as $j_{NO_3} = 42\,A\,m^{-2}$. Using the identical procedure and considering the concentration of oxygen in the solution of $10\,mg\,dm^{-3}$, the limiting current density for the oxygen reduction was evaluated as $j_{O_2} = 0.46\,A\,m^{-2}$.

These values explain the basic features of the dependencies shown in Fig. 2. Using current density of $20\,A\,m^{-2}$ the mass-transfer-limiting current density is reached at the nitrate bulk concentration of approximately $470\,mg\,dm^{-3}$. This corresponds well to the linear decrease in nitrate concentration in time observed for this concentration range. After concentration decreases below this level its further decrease is slowed down by the parasitic reaction (hydrogen evolution). The dependence of the cathode potential observed corresponds well to this fact. During the first period of the time the chronopotentiometric curve shows a delay in potential range around $-1.00\,V$. The slow potential shift to the more cathodic values corresponds to the gradual change in the ratio between the extents of the two successive nitrate reduction steps. As shown in the previous study [15], in the first step nitrate is reduced to nitrite. This reaction, however, requires two only electrons. From this, it follows that not all the electrical charge can be consumed by this reduction mechanism step. Exceeding charge is used to reduce nitrite to ammonium. This electrolysis period is characterised by the steep increase in the nitrite concentration of the electrolyte solution. As the nitrate concentration decreases, the reduction of nitrites to ammonium gradually proceeds to a greater extent. Corresponding to this, the cathode potential shifts to more cathodic values and the nitrite concentration in the solution starts to decrease. Once the limiting current density value calculated for complete nitrate reduction to ammonium is exceeded, there is a steep increase in potential to the value of $-1.14\,V$, where the parasitic reaction—hydrogen evolution—takes place. As discussed in the theoretical part of this study, hydrogen evolution inhibits the nitrate reduction on the cathode surface. This is why the nitrite concentration in the solution reaches the limiting value. With increasing cell current load the limiting current density value is exceeded at the very start of electrolysis. This results in a much lower nitrite concentration maximum at the start of electrolysis and in the more cathodic Cu electrode potential. Thereupon the hydrogen evolution intensity increases and consequently the nitrate concentration decrease on electrical charge spent becomes slower and its limiting value increases.

As discussed in a previous study [14], addition of Cu ions to the solutions enhances the electrocatalytic activity of the cathode. This was also proven by the polarisation measurements on the Cu rotating disk electrode (RDE) [15]. It was observed in the present work that current density on nitrate reduction to nitrite increases substantially by the addition of Cu ions to the electrolyte, see Fig. 3. Firstly, we can clearly observe less cathodic electrode potential in comparison to electrolysis without the addition of Cu ions to the electrolyte. Corresponding to this, the nitrite reaches steady concentration several times higher. This is in agreement with the voltammetric experiments [15] where the cathodic peak corresponding to the nitrate to nitrite reduction was enhanced significantly by the addition of Cu ions. Since the process is limited by the mass-transfer from the bulk to the electrode surface, the increase in the reduction current yield cannot be explained by the renewal of the electrocatalytic activity only. Mass-transfer has to be enhanced as well. This is probably because the real cathode surface area is enlarged by the continuous Cu deposition on its surface and by the increase in surface roughness. The continuous renewal of cathodic electrocatalytic activity explains the lower nitrate concentration limit at the end of electrolysis. The continuously renewed surface, however, does not influence the nitrite reduction reaction.

By substituting superficial electrolyte velocity in the inter-electrode space of $v = 3.6 \times 10^{-2}\,m\,s^{-1}$ and fluidised bed porosity of $\varepsilon = 0.6$ in Eqs. (12)–(14), the following values of the mass-transfer coefficients were evaluated: $k_{NO_3} = 3.0 \times 10^{-5}\,m\,s^{-1}$ and $k_{O_2} = 3.4 \times 10^{-5}\,m\,s^{-1}$ for the cell with a fluidised bed of inert particles in the inter-electrode space. The limiting cathode current densities

for the nitrate reduction at the beginning of electrolysis ($1\,g\,NO_3^-\,dm^{-3}$) have, thus, the values $j_{NO_3} = 373\,A\,m^{-2}$ and $j_{O_2} = 4.1\,A\,m^{-2}$. The linear course of the nitrate concentrations in the time of electrolysis down to the concentration of approximately $100\,mg\,dm^{-3}$, shown in Fig. 4, corresponds well to this important mass-transfer enhancement. It exhibits a linear shape, proving the process is dependent on a parameter different from the nitrate mass-transfer. Correspondingly, the current yield remains approximately constant in this region with some deviations at the first experimental point caused predominantly by a cathode surface conditioning. Furthermore, the values of the nitrite concentration in the electrolyte correspond to an increase in mass-transfer intensity when compared to the simple plate-electrode cell. Soon after electrolysis starts it reaches a maximum. Contrary to the cell without a fluidised bed, the maximum is most apparent at the current density of 40 and $80\,A\,m^{-2}$. This is probably because, in the case of the lowest current density $20\,A\,m^{-2}$, an important part of the total electrical charge is consumed by the oxygen reduction reaction. The chronopotentiometric curves show behaviour similar to the simple plate-electrode cell. Only the potential steps corresponding to the commencement of the parasitic reaction are more pronounced in this case. This agrees with the higher mass-transfer rate, which causes more sudden electrode reactions changes and can be seen most clearly for the current density of $20\,A\,m^{-2}$. Here potential remains almost constant for the first $12\,kC\,dm^{-3}$, which is a range, where the current density used is lower than that limited by the mass-transfer. During this period nitrite concentration in the solution remains approximately constant. This indicates that the kinetics of the nitrate to nitrite reduction and its subsequent reduction to ammonium has reached a steady state value equal for both of these mechanism steps. Once the current density limiting value has been exceeded, the electrode potential is shifted to the more cathodic value and the nitrite reduction kinetics increases. In a subsequent step, the hydrogen evolution reaction takes place, as discussed above. With enhanced current density these processes are less apparent because the current density of the nitrate to nitrite reduction apparent on the polarisation curve has been exceeded [15]. This causes the potential to start at more cathodic values and its changes in the course of electrolysis are less apparent. Moreover, the dependence of the nitrite concentration on the charge spent shows a distinct maximum and in these cases, the constant plateau is absent. These results from the fact, that after the first portion of this intermediate product has formed, the kinetics of its reduction prevails over its formation because of the current density used and the corresponding cathode potential. The electrolysis shows practically identical behaviour for current densities $j \leq 120\,A\,m^{-2}$. Using higher current density their behaviour deviates significantly. This corresponds to the previously made statement about the kinetics current density representing the second limitation of the nitrate reduction process [15]. It was observed in [15] that at current densities higher than $130\,A\,m^{-2}$ hydrogen evolution takes place at the copper cathode surface and efficiency of the nitrate reduction deteriorates.

The superficial electrolyte flow rate of $4.2 \times 10^{-2}\,m\,s^{-1}$ and mean copper particle diameter of $3 \times 10^{-3}\,m$ were considered for the evaluation of the mass-transfer in the static 3D cathode. Using Eqs. (21) and (22) for the NO_3^- and O_2, mass-transfer coefficients of $k_{NO_3} = 8.3 \times 10^{-5}\,m\,s^{-1}$ and $k_{O_2} = 9.4 \times 10^{-5}\,m\,s^{-1}$, respectively were calculated. The superficial limiting current densities of $\bar{j}_{NO_3} = 11\,000\,A\,m^{-2}$ and $\bar{j}_{O_2} = 120\,A\,m^{-2}$ for the nitrates and dissolved oxygen reduction, respectively were evaluated to correspond to these electrolysis parameters. Despite the high mass-transfer-limiting current density, this type of cell provided only poor current efficiency, as shown in Fig. 5. This is caused by the irregular potential and local current densities distribution across the stationary cathode bed. From this point of view three regions of the 3D cathode can be distinguished. These are schematically presented in Fig. 7. In region A, the local values of the current density are almost zero. Current flowing here is consumed mainly by the oxygen reduction reaction. In region B, the current density exceeds the oxygen reduction limiting current density. The next electrode reaction to take place is the reduction of nitrate to nitrite. In the last region C, the local current density value increases steeply above the nitrate-limiting current density and most of the electrical charge is consumed by the hydrogen evolution, i.e. the parasitic cathodic reaction. The major part of the electrical charge is typically consumed in regions B and C. Since the cell operates in a flow-by arrangement, different fractions of electrolyte pass through different parts of the cathode. This leads to the high nitrite concentration observed in the electrolyte and to the generally low current yield. On the other hand, however, current yields increase with increasing superficial current density. This is due to the expansion of region B and the gradual diminution of region A of the 3D cathode

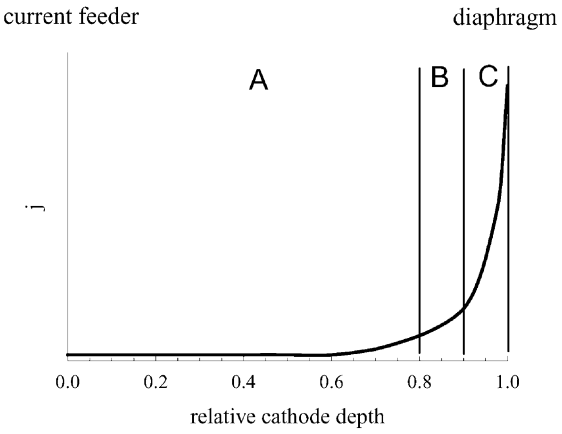

Fig. 7. Schematic current density course across the packed bed cathode.

with increasing current load. Another unusual feature is the lowest current efficiency observed for the lowest current density used. This can be explained by the thermodynamically preferred cathodic reduction of the oxygen dissolved in the electrolyte solution. Limiting current density for this process reaches almost a half of the lowest current density studied ($100\,A\,m^{-2}$). Moreover, at the lowest current density potential distribution across the electrode is quite uniform and lies in the region of the oxygen reduction reaction (differences between the regions A to C are not important). This results in the important decrease in efficiency of the electrolysis with respect to the NO_3^- reduction.

The VMPB reactor was operated using the superficial electrolyte flow rate of $1.6 \times 10^{-3}\,m\,s^{-1}$. In this particular case, a uniform Cu particle size distribution was used across the individual cathode drums. The mean particle diameter was $2 \times 10^{-3}\,m$. Using these parameters, the mass-transfer coefficient values of $k_{NO_3} = 1.5 \times 10^{-5}\,m\,s^{-1}$ and $k_{O_2} = 1.7 \times 10^{-5}\,m\,s^{-1}$ were calculated, neglecting the fact that the solution was additionally mixed by the cathode drum rotation. This corresponds to the cell current for the nitrate reduction of 267 A and for the oxygen reduction of 1.4 A. Comparing these values with the packed bed cathode, it can be seen that, without rotation, the VMPB cell would provide a mass-transfer density lower than that of the packed bed cathode. This is mainly due to the lower electrolyte superficial flow rate. Taking into account the cell rotation, the mass-transfer coefficients of the packed bed and VMPB cells may be considered to be comparable. As shown in Fig. 6, the VMPB cell, however, provides superior efficiency of nitrate reduction. Strong deterioration of the electrocatalytic activity at the current load of 25 A indicates that the current density distribution across the 3D cathode again plays an important role. The question remains the high current yield when compared to the packed bed cathode. One possible explanation is the different cathode configuration, which in the VMPB cell, is flow-through. This means that the entire electrolyte has to pass through all three zones of the current distribution across the 3D electrode. Moreover, the anodes are localised on both sides of the cathode drums, which results in sections B and C (see Fig. 7) appearing symmetrically on both ends of the cathode drum. The flow of the electrolyte through all three electrode parts results in the nitrite being more efficiently reduced in part C and its concentration decreasing with time to zero. An additional parameter may be the mechanical renewal of the Cu particle surface of the cathode. This helps to maintain the surface of the cathode catalytically active even if the kinetic limiting current density is exceeded.

High mass-transfer conditions together with the above-mentioned effects cause a sharp increase in NO_2^- concentration during the first $10^4\,C\,dm^{-3}$ of electrolysis. A further reduction of nitrite takes place after the decrease in nitrate concentration below a mass-transfer-limiting value. This coincides with a delay in the increase of ammonia concentration in the initial electrolysis period.

6. Conclusions

These results document the importance of the mass-transfer phenomenon and regular potential and current density distribution across the 3D electrode for the efficiency of the electrochemical nitrate reduction. The optimal choice seems to be the cell providing intensive mass-transfer and at the same time continuous renewal of the cathode surface. One way is the addition of Cu ions to the electrolyte. This, however, introduces Cu ions and Cu salt suspension into the solution, which may in accidental cases lead to a leakage into the drinking water. The alternative way of cathodic mechanical friction is, therefore, preferable. In the present study, this was provided either by the fluidised glass particles or by the rotation of the particle cathode. As documented clearly by the results presented, NO_3^- is reduced practically quantitatively to NH_3. No reduction to N_2, which is often referred to in the literature, was proven here.

Acknowledgements

The financial support of this research by the Grant Agency of the Czech Republic, Project number 104/99/0433, and by the Ministry of Education, Youth and Sports, Project number CEZ: MSM223100001, is gratefully acknowledged.

References

[1] I. Bogardi, R.D. Kuzelka (Eds.), Nitrate Contamination: Exposure, Consequence, and Control, Springer, Berlin, 1991
[2] H. Roques, Chemical Water Treatment Principles and Practice, VCH, New York, 1996, p. 541
[3] O. Strebel, W.H.M. Duynisveld, J. Boettcher, Agric. Ecosyst. Environ. 26 (1989) 189.
[4] J.O'M. Bockris, J. Kim, J. Appl. Electrochem. 27 (1997) 623.
[5] J.D. Genders, D. Hartsough, D.T. Hobbs, J. Appl. Electrochem. 26 (1996) 1.
[6] P. Pitter, Hydrochemistry, SNTL, Prague, 1990 (in Czech).
[7] V. Kadlec, Separation and Analytical Methods in Environmental Protection, Edition Macro, Vol. M-21, Prague, 1996 (in Czech)
[8] N. Strnadová, V. Janda, Z. Matějka, E. Říhová, Vodní hospodářství 6 (1991) 209.
[9] S. Hrold, K.D. Vorlop, T. Tacke, M. Sell, in: Proceedings of the 1st European Workshop Meeting on Environmental Industrial Catalysis, 9–10 November 1992, Louvain-la-Neuve, Belgium.
[10] J.O'M. Bockris, J. Kim, J. Electrochem. Soc. 143 (1996) 3801.
[11] J. Kaczur, D. Cawlfield, K. Woodart Jr., US Patent Appl. 5,376,240 (1994).
[12] W.J. Plieth, in: A.J. Bard (Ed.), Encyclopedia of Electrochemistry of the Elements, Marcel Dekker, Vol. VIII, 1978, Chapter 5.
[13] N. Chebotareva, T. Nyokong, J. Appl. Electrochem. 27 (1997) 975.
[14] M. Paidar, I. Roušar, K. Bouzek, J. Appl. Electrochem. 29 (1999) 611.
[15] K. Bouzek, A. Sadílková, M. Paidar, H. Bergmann, J. Appl. Electrochem., submitted for publication.
[16] G. Horányi, E.M. Rizmayer, J. Electroanal. Chem. 140 (1982) 347.

[17] G. Horányi, E.M. Rizmayer, J. Electroanal. Chem. 143 (1983) 323.
[18] S. Ureta-Zanartu, C. Yanez, Electrochim. Acta 42 (1997) 1725.
[19] N.G. Carpenter, D. Pletcher, Anal. Chim. Acta 317 (1995) 287.
[20] S. Cattarin, J. Appl. Electrochem. 22 (1992) 1077.
[21] Y. Xiang, D. Zhou, J.F. Rushling, J. Electroanal. Chem. 424 (1997) 1.
[22] H. Li, D.H. Robertson, J.Q. Chambers, D.T. Hobbs, J. Electrochem. Soc. 135 (1988) 1154.
[23] H. Li, J.Q. Chambers, D.T. Hobbs, J. Appl. Electrochem. 18 (1988) 454.
[24] M. Paidar, L. Jelínek, K. Bouzek, Z. Matějka, Water Environ. Res., submitted for publication.
[25] K. Hertwig, H. Bergmann, A. Rittel, Elektrolyseapparat mit Partikelkathoden, DE 4210917, 28 January 1993.
[26] I. Roušar, J. Hostomský, V. Cezner, B. Štverák, J. Electrochem. Soc. 118 (1971) 881.
[27] K. Bouzek, J. Palmer, I. Roušar, A.A. Wragg, Electrochim. Acta 41 (1996) 583.
[28] A. Storck, M. A Enriquez-Granados, M. Roger, Electrochim. Acta 27 (1982) 303.
[29] I. Colquhoun-Lee, J. Stepanek, Chem. Eng. 282 (1974) 108.
[30] J.S. Newman, W. Tiedemann, Flow-through porous electrodes, in: H. Gerischer, C.W. Tobias (Eds.), Advances in Electrochemistry and Electrochemical Engineering, Vol. 11, Wiley, New York, 1978.
[31] M. Malát, Inorganic Absorption Photometry, Academia, Prague, 1973 (in Czech).
[32] EEC Council Directive 98/83/EC.